Synthesis and luminescence properties of Dy^{3+} IONS phosphate based Glasses for White LEDs

T. Chengaiah[1]*

[1]Department of Physics, Sri Venkateswara University, Tirupati-517502, A.P., INDIA

*Corresponding author : chengaiahphysics@gmail.com

ABSTRACT

A series of dysprosium (Dy^{3+})-doped phosphate glasses with varying Dy_2O_3 concentrations were successfully synthesized via the conventional melt-quenching technique. X-ray diffraction (XRD) analysis confirmed the amorphous nature of all prepared samples, while elemental mapping verified the homogeneous distribution of constituent elements throughout the glass matrix.Optical absorption spectra were analyzed using Judd–Ofelt (J–O) theory, and the calculated intensity parameters (Ω_2, Ω_4, Ω_6) followed the order $\Omega_2 > \Omega_6 > \Omega_4$. This trend suggests a highly asymmetric local environment and significant covalent bonding character around the Dy^{3+} ions.Photoluminescence (PL) studies under 350 nm excitation revealed characteristic emissions corresponding to the $^4F_{9/2} \rightarrow {}^6H_j$ transitions, including a weak red emission ($^4F_{9/2} \rightarrow {}^6H_{11/2}$), along with intense blue ($^4F_{9/2} \rightarrow {}^6H_{15/2}$) and yellow ($^4F_{9/2} \rightarrow {}^6H_{13/2}$) bands. Lifetime measurements of the $^4F_{9/2}$ excited state indicated that the emission intensity reached a maximum at 0.5 mol% Dy_2O_3, beyond which concentration quenching effects became prominent. Furthermore, the near-white light emission characteristics were evaluated through the yellow-to-blue (Y/B) intensity ratio, correlated color temperature (CCT), and Commission Internationale de l'Éclairage (CIE) chromaticity coordinates, confirming the potential applicability of the prepared glasses in solid-state lighting devices.

Keywords: optical absorption, Photoluminescence, Dy^{3+} ions, white LEDs, Radiative transition probability.

INTRODUCTION

Rare-earth (RE) ion-doped glasses have gained considerable attention owing to their unique optical properties arising from intra-4f electronic transitions, which are effectively shielded by the outer filled electron shells[1,2]. This shielding results in sharp emission bands and high color purity, making these materials highly suitable for photonic applications. Compared to ceramics and phosphors, glass hosts offer several advantages, including superior chemical stability, ease of fabrication, the ability to accommodate higher concentrations of RE ions, and cost-effective processing[3,5]. Consequently, RE-doped glasses have been widely explored for applications such as solid-state lasers, optical amplifiers, field-emission displays, sensors, infrared-to-visible up-conversion devices, nonlinear optical systems, and white light-emitting diodes (w-LEDs)[6,9].Among various RE ions, dysprosium (Dy^{3+}) has emerged as a promising activator due to its characteristic emission features in the visible region. In particular, Dy^{3+} exhibits intense blue ($^4F_{9/2} \rightarrow {}^6H_{15/2}$, ~480 nm) and yellow ($^4F_{9/2} \rightarrow {}^6H_{13/2}$, ~575–590 nm) transitions[10-12], which can combine to produce near-white light emission. This property makes Dy^{3+}-doped systems highly attractive for solid-state lighting and w-LED applications. Furthermore, Dy^{3+} ions are known to exhibit high emission intensity, excellent color purity, and favorable quantum

efficiency when incorporated into suitable glass matrices[13-16]. Therefore, the development of optimized host compositions for Dy^{3+}-doped glasses is essential for enhancing their optical performance in visible photonic devices.Various glass systems, including borate, phosphate, silicate, and tellurite hosts, have been extensively investigated to tailor the luminescent properties of RE ions. Among these, borotellurite glasses represent a unique class of materials that combine the excellent glass-forming ability and structural stability of borate networks with the superior optical characteristics of tellurite glasses. Borate glasses possess a highly connected three-dimensional network formed by structural units such as diborate, triborate, tetraborate, and pentaborate groups, which contribute to their thermal stability and mechanical strength. On the other hand, tellurite glasses are characterized by low phonon energy (800–900 cm^{-1}), high refractive index, and high solubility for RE ions, thereby minimizing non-radiative losses and enhancing luminescence efficiency[17-19]. As a result, borotellurite glasses exhibit excellent optical transparency, chemical durability, and thermal stability, making them suitable candidates for applications in lasers, nonlinear optics, and w-LED technologies.The incorporation of suitable network modifiers further enhances the structural and optical performance of these glass systems. For instance, Al_2O_3 improves network connectivity by increasing cross-link density, thereby enhancing thermal and mechanical stability. Similarly, MgO modifies the local environment around RE ions, reducing ion clustering and improving both optical transparency and structural integrity. The presence of such modifiers strengthens the glass network and suppresses phonon-assisted non-radiative relaxation processes, ultimately leading to improved luminescence efficiency[20-22].

EXPERIMENITAL

MATERIALS

Phosphate glasses doped with varying concentrations of Dy^{3+} ions were synthesized using the conventional melt-quenching technique. High-purity (≥99.9%) $Al(PO_3)_3$, KH_2PO_4, CaF_2, and Dy_2O_3 (99.99%) powders were accurately weighed with a precision of ±0.0001 g and thoroughly mixed in appropriate stoichiometric proportions. Approximately 10 g of each batch composition was melted in a platinum crucible at 1150 °C for about 1 hour to ensure complete homogenization.The molten glass was then rapidly quenched and subsequently annealed for 12 hours to relieve internal thermal stresses induced during the quenching process, followed by slow cooling to room temperature. The prepared glass samples were designated as PKAlMDy01, PKAlMDy05, PKAlMDy10, PKAlMDy15, and PKAlMDy20, corresponding to Dy_2O_3 concentrations of 0.1, 0.5, 1.0, 1.5, and 2.0 mol%, respectively.

Instrumentation and Analytical Methods

The optical and physical properties of the PKAlMDy glass samples were evaluated using standard characterization techniques. The density of each specimen was measured following Archimedes' principle with distilled water as the immersion medium. The refractive index was determined using an Abbe refractometer with a sodium vapor light source (λ = 589.3 nm) and 1-bromonaphthalene as the contact liquid.To confirm the amorphous structure, X-ray diffraction (XRD) analysis was carried out using a RIGAKU diffractometer within the 2θ range of 5°–90°. Optical absorption spectra in the UV, visible, and near-IR regions were obtained using a Jasco V-570 spectrophotometer. Photoluminescence excitation and emission spectra were recorded

using an Edinburgh Instruments FLS980 spectrofluorometer at an excitation wavelength of 350 nm and a spectral resolution of 1 nm. The lifetime decay of the $^4F_{9/2}$ excited state of Dy^{3+} ions was also measured using the same setup. All experiments were carried out under ambient conditions.

RESULTS & DISCUSSION

X-ray Diffraction (XRD) Analysis

Figure 1 displays the X-ray diffraction (XRD) patterns of the PKAlMDy glass specimens. All samples exhibit a broad, diffused hump without any sharp Bragg reflections, confirming their non-crystalline (amorphous) structure. The diffraction measurements were recorded at room temperature using a RIGAKU XRD instrument over the 2θ scan range of 10° to 70°.The appearance of a large hump in the lower scattering region is characteristic of non-crystalline materials and is due to the long-range structural chaos and short-range atomic groupings found in amorphous glasses[25]. The absence of prominent Bragg reflections suggests that no crystalline phases occur during the glass formation process, even after Dy_2O_3 inclusion. These observations demonstrate that Dy^{3+} ions successfully incorporate into the borotellurite network without causing devitrification or phase separation. As a result, the acquired XRD patterns significantly support the amorphous nature and structural homogeneity of the produced PKAlMDy glass system.

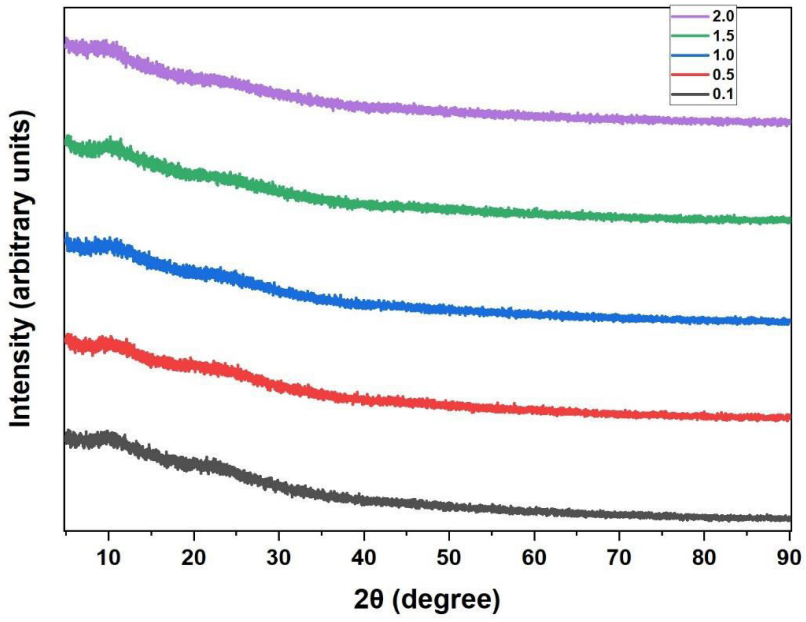

Figure 1. XRD spectra of Dy^{3+} doped PKAlM glasses.

Spectral Absorption Features and Judd–OfeltModelling

The optical absorption spectra of the Dy^{3+}-doped borotellurite glass samples were measured over the 300–1800 nm wavelength range in order to study the characteristic electronic transitions

originating from the $^6H_{15/2}$ ground state of Dy^{3+} ions. The recorded spectra, shown in Figures 2(a) (VIS) and 5(b) (NIR), show well-defined absorption bands corresponding to the intra-4f transitions characteristic of trivalent dysprosium. Absorption peaks at 346, 382, 426, 448, and 473 nm are caused by the $^6H_{15/2} \rightarrow {}^6P_{5/2}$, $^4I_{13/2}$, $^4G_{11/2}$, $^4I_{15/2}$, and $^4F_{9/2}$ transitions, respectively. The near-infrared region has transitions at 752, 806, 898, 1088, 1264, and 1657 nm. These correspond to the $^6H_{15/2} \rightarrow {}^6F_{3/2}$, $^6F_{5/2}$, $^6F_{7/2}$, $^6H_{7/2}$, $^6F_{11/2}$, and $^6H_{11/2}$ levels.

Among these, the band at 1264 nm (6H15/2→6F11/2) exhibits the highest intensity, indicating a hypersensitive transition associated with the asymmetric and covalent nature of Dy–O coordination in the glass matrix. The sharp and well-defined absorption peaks, without noticeable splitting, confirm a homogeneous distribution of Dy^{3+} ions within the amorphous network [23].The experimental oscillator strengths (f_exp) for the detected transitions were calculated from the integrated absorption cross-section, while the theoretical values (f_cal) were obtained using the Judd–Ofelt (J–O) theoretical model. A comparison of these values, presented in Table 2, reveals good agreement between experimental and theoretical results, with only minor deviations attributed to weak transition probabilities and the neglect of higher-order relativistic effects. The root mean square (RMS) deviation (δrms = ±0.54×10−6) lies within acceptable limits, confirming the reliability of the fitting procedure.

The Judd–Ofelt parameters (Ω_2, Ω_4, and Ω_6) serve as key indicators of the symmetry and chemical environment experienced by Dy^{3+} ions within the glass network.The relatively higher Ω2 value indicates a strong covalent character and significant asymmetry in the Dy–O coordination, accounting for the hypersensitive transition observed in the NIR region. The trend Ω2>Ω6>Ω4 suggests that short-range interactions dominate over long-range field effects in the glass matrix [24].Overall, the high oscillator strengths and pronounced hypersensitive transitions confirm that Dy^{3+} ions occupy low-symmetry, covalently bonded sites within the borotellurite framework. The results indicate that these glasses are potential candidates for photonic and white-light applications due to their effective f–f transitions and desirable optical features.

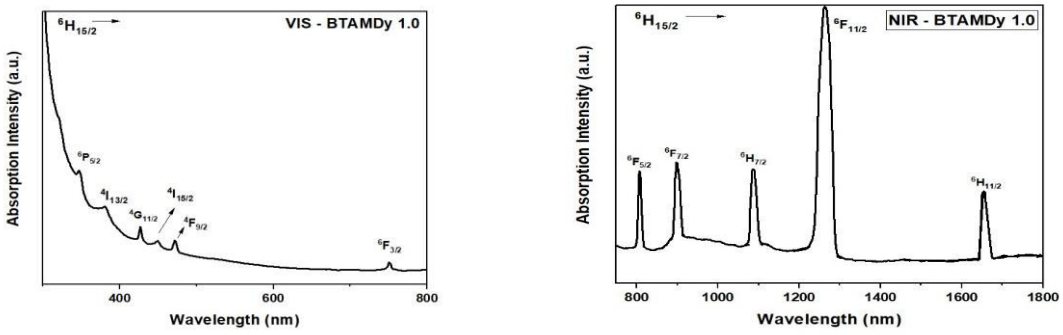

(a) (b)

Figure 2. Optical absorption spectra of Dy^{3+} doped PKAlM glasses.

Excitation Study

Figure 3 displays the excitation spectra of Dy^{3+} doped borotellurite glasses from 300-700 nm, with emission measured at 575 nm. The spectra show four different excitation bands at 323, 350, 364, and 386 nm. These bands correspond to the Dy^{3+} ion transitions $^6H_{15/2} \rightarrow {}^4M_{17/2}$, $^6H_{15/2} \rightarrow {}^6P_{7/2}$, $^6H_{15/2} \rightarrow {}^6P_{5/2}$, and $^6H_{15/2} \rightarrow {}^4I_{13/2}$. The $^6H_{15/2} \rightarrow {}^6P_{7/2}$ transition at 350 nm has the highest intensity and dominates the excitation process. This wavelength was chosen to excite the Dy^{3+} ions, and the corresponding emission spectra for all glass samples were subsequently recorded. The excitation intensity progressively rises with the concentration of Dy^{3+} until it reaches 1.0 mol%, after which it slightly decreases [25]. This pattern implies that at higher dopant levels, concentration quenching occurs as a result of non-radiative energy transfer between closely spaced Dy^{3+} ions. The glass network's structural disorder and the fluctuating local ligand environments surrounding Dy^{3+} ions are reflected in the broadening of excitation bands. The distinct and abrupt peaks support the intra-configurational 4f–4f character of Dy^{3+} transitions, which are only marginally impacted by the matrix environment. A pure electronic transition is shown by the conspicuous band at 350 nm, which also reveals details about the local symmetry surrounding the Dy^{3+} sites in the glass matrix [26]. The acquired spectral pattern confirms that Dy^{3+} ions were successfully incorporated into the borotellurite network without altering its amorphous nature, since it is compatible with previously reported Dy^{3+} doped oxide and tellurite glasses.

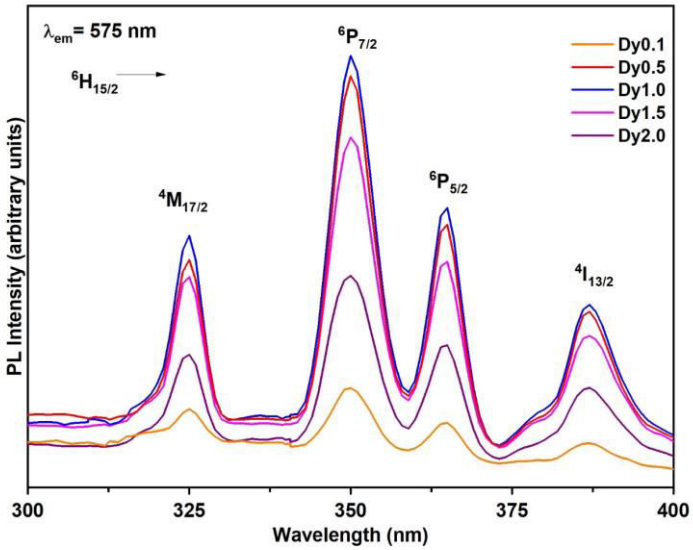

Figure 3. Excitation spectra monitored at 575 nm emission.

Emission Spectra

Figure 4 presents the photoluminescence spectra of Dy^{3+}-doped borotellurite glass samples under 350 nm excitation. The spectra reveal three distinct emission peaks located near 483, 575, and 665 nm, which are assigned to the $^4F_{9/2} \rightarrow {}^6H_{15/2}$, $^4F_{9/2} \rightarrow {}^6H_{13/2}$, and $^4F_{9/2} \rightarrow {}^6H_{11/2}$ electronic transitions of Dy^{3+} ions, respectively.The blue emission at 483 nm originates from a magnetic dipole transition, whereas the yellow emission at 575 nm arises from an electric dipole transition that is highly sensitive to the local field asymmetry around the Dy^{3+} ions[27] . The dominance of the yellow band over the blue one indicates that Dy^{3+} ions occupy sites without inversion symmetry in the borotellurite glass matrix.

As the Dy^{3+} concentration increases, the emission intensity steadily rises and reaches its maximum at 1.0 mol%, after which it drops due to concentration quenching. This reduction in intensity at higher dopant levels is likely caused by non-radiative energy transfer processes, including cross-relaxation and multiphonon interactions between closely spaced Dy^{3+} ions. Therefore, 1.0 mol% is identified as the optimum dopant level for achieving maximum luminescence efficiency in this glass system[28].

The radiative properties, including transition probability(A_R), stimulated emission cross-section (σ_{se}),radiative lifetime (τ_R), gain bandwidth (σ_{se} x $\Delta\lambda_p$), and optical gain (σ_{se} x τ_R) were calculated based on Judd–Ofelt analysis[29], and the obtained values are presented in Table 4.The results clearly indicate that the yellow emission transition, $^4F_{9/2} \rightarrow {}^6H_{13/2}$ at 575 nm, exhibits larger $\sigma_{se}$and gain bandwidth values than the blue emission transition, $^4F_{9/2} \rightarrow {}^6H_{15/2}$ at 483 nm.Among all compositions, the PKAlMDy1.0 glass exhibits the highest A_R (2.74 $s^{-1} \times 10^3$), σse (11.5 $\times 10^{-21}$ cm^2), gain bandwidth (3.87 $\times 10^{-27}$ cm^3), and optical gain (10.6 $\times 10^{-24}$ cm^2 s), confirming its superior radiative efficiency and enhanced stimulated emission probability.

At higher Dy^{3+} concentrations (≥ 1.5 mol %), the decrease in these parameters results from energy migration and non-radiative loss channels among adjacent Dy^{3+} ions[30]. Consequently, 1.0 mol % Dy^{3+} is established as the optimum concentration for achieving maximum optical gain and emission efficiency. The excellent gain characteristics and dominant yellow emission suggest that Dy^{3+}-activated glasses are promising materials for visible laser and photonic amplifier applications, particularly in the yellow spectral region.

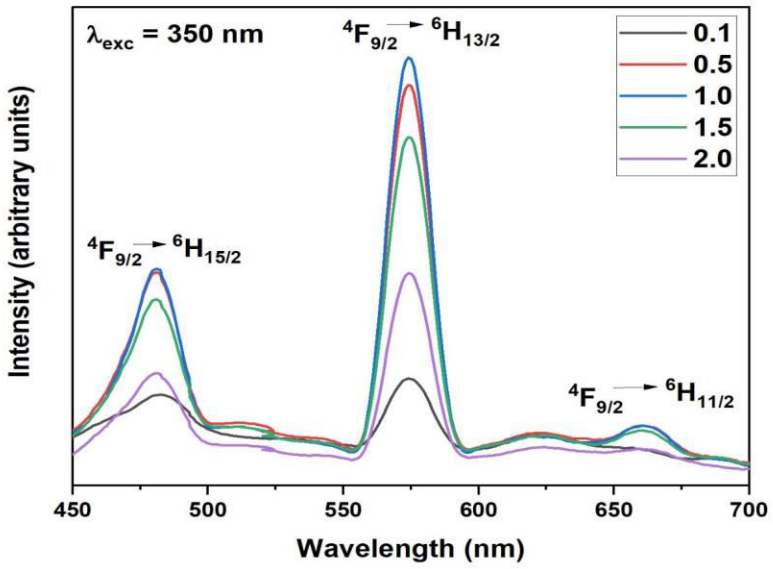

Figure 4. Emission spectra under 350 nm excitation

Lifetime Analysis

Figure 5 presents the decay profile corresponding to the excited $^4F_{9/2}$ level of Dy^{3+} ions in the borotellurite glass system under 350 nm excitation. The decay behavior deviates from a single-exponential trend, indicating the presence of multiple local coordination environments surrounding Dy^{3+} ions within the glass matrix. This suggests that Dy^{3+} ions may occupy different sites with varying ligand fields, leading to heterogeneous relaxation dynamics.A property of highly polarizable glass systems, this divergence is mostly caused by energy migration and cross-relaxation events between neighboring Dy^{3+} ions[31]. As the concentration of Dy^{3+} increases, the average lives tested experimentally gradually decrease. The lifetime is around 620 µs at 0.1 mol%, lowers to about 553 µs at 0.5 mol%, and then declines even more to 337 µs at 1.0 mol%. The lifetime rapidly decreases beyond this critical concentration, reaching about 298 µs for 1.5 mol% Dy^{3+} and 290 µs for 2.0 mol% Dy^{3+}. Concentration quenching brought on by non-radiative energy transfer between Dy^{3+} ions is responsible for this ongoing decrease. Dominant radiative transitions are produced at lower concentrations because Dy^{3+} ions stay well separated. Shorter decay durations result from cross-relaxation and multiphonon interactions becoming important when the ions get closer with increased doping[32].

The glass doped with 1.0 mol% Dy^{3+} shows the best balance between lifespan and luminescence intensity among all compositions, suggesting effective energy use prior to quenching. These findings verify that the decay properties of Dy^{3+}-doped borotellurite glasses are highly influenced by the dopant concentration and that the optimal dopant concentration for steady and effective yellow emission performance is 1.0 mol%.

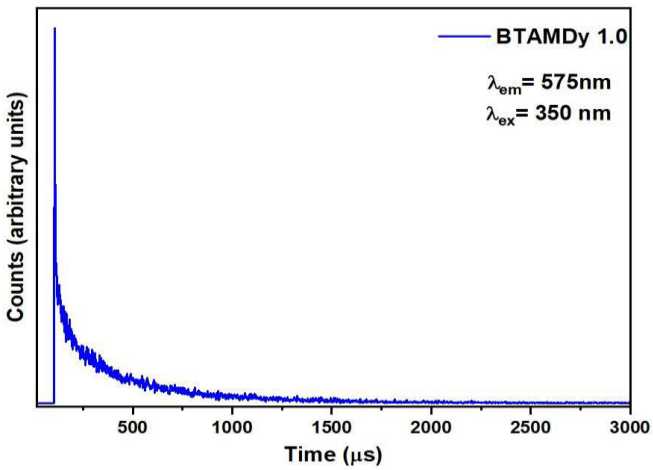

Figure 5. Lifetime decay profile of Dy^{3+} doped PKAlM glasses.

CONCLUSION

A novel set of Dy^{3+}-doped glasses was synthesized using the conventional melt-quenching technique, and their structural, optical, and photoluminescence characteristics were comprehensively investigated.which showed distinct f–f transitions. Reliable intensity parameters (Ω_2, Ω_4, and Ω_6) were obtained by Judd–Ofelt analysis. The pattern $\Omega_2 > \Omega_6 > \Omega_4$ suggested a strong covalent bonding environment and notable local asymmetry around Dy^{3+} ions. The emission spectra were dominated by the $^4F_{9/2} \rightarrow {}^6H_{13/2}$ transition at 575 nm, which produced bright yellow luminescence. The blue emission was caused by the $^4F_{9/2} \rightarrow {}^6H_{15/2}$ transition at 483

nm. The emission intensity increased with Dy^{3+} concentration and reached its maximum at 1.0 mol%. Beyond this level, further doping led to a reduction in luminescence due to concentration quenching, which is attributed to non-radiative energy transfer processes occurring between closely spaced Dy^{3+} ions.This behavior was corroborated by the matching lifetime studies, which demonstrated a progressive decay time decrease with increasing dopant concentration. According to the CIE chromaticity evaluation, all samples exhibited emission coordinates lying close to the white-light region. The glass system's appropriateness for next-generation luminous materials is highlighted by its steady colorimetric features, efficient radiative parameters, and high asymmetry ratio.

REFERENCES

1. B. R. Judd, *Physical review*, **127**, 750(1962), https://doi.org/10.1103/PhysRev.127.750
2. G. S. Ofelt, *TheJournal of Chemical Physics*, **37**,511(1962),
3. S. O. Adeleye, A. A. Adeleke, P. Nzerem, A. I. Olosho, E. N. Anosike-Francis, T. S. Ogedengbe, J. A. Okolie, *Trends in Sciences*, **21(12)**, 8759(2024),
4. V. Kumar, S. Kumari, S. Malik, T. Ravita Sharma, A. Prasad, & A. S. Rao, *Journal of Fluorescence*,35, 7385(2025),
5. C. Julien, M. Massot, W. Balkanski, A. Krol, & W. Nazarewicz, *Materials Science and Engineering: B*, **3**,307(1989),
6. V. P. Tuyen, B. Sengthong, V. X. Quang, P. Van Do, H. Van Tuyen, L. X. Hung & B. T. Huy, *Journal of Luminescence*, **178**, 27(2016),
7. V. Chandrappa, Ch. Basavapoornima, V. Venkatramu, D. Shobha Rani, J. Kaewkhao, W. Pecharapa,C.K.Jayasankar,*Optik*,**266,**169583(2022),
8. Jose A. Jimenez, VinodHegde, C.S. DwarakaViswanath, A. Richard, ACS Physical Chemitry Au, **4**, 720 (2024),
9. A. Górny, M. Kuwik, W. A. Pisarski, & J. Pisarska, *Materials*, **13**,5022(2020),
10. N. Mahingsa, W. Rachniyom, K. Kirdsiri, & N. Srisittiposakun, *SuanSunandhaScience and Technology Journal*,**12,** 32(2025), https://doi.org/10.53848/ssstj.v12i1.1034
11. S. Khondara, P. Yasaka, K. Boonin, N. Intachai, S. Kothan, H. J. Kim, & J. Kaewkhao, *Radiation Physics and Chemistry*, **237**, 113007(2025),
12. Y. Zhang, & Z. Zhu, *Journal of Non-Crystalline Solids*,**627**, 122826(2024),
13. V.P. Tuyen ,B. Sengthong , V.X. Quang , P. Van Do , H. Van Tuyen ,L.X. Hung, N.T. Thanh,,M. Nogami, T. Hayakawa , B.T. Huy,*Journal of Non-Crystalline Solids,* **178***,* 27(2016).
14. T. Komatsu, & V. Dimitrov, *International Journal of Applied Glass Science*, 11, 253 (2019),
15. V. A. G. Rivera, I. C. Pinto, R. Falci, V. Fuertes, & Y. Messaddeq, *Journal of Alloys and Compounds*, **976**,173182(2024),
16. A. M. Abdelghany, & H. A. ElBatal, *Materials & Design*, **89**,568(2016).
17. M. I. Sayyed, A. H. Almuqrin, T. A. Hanafy, & M. Elsafi, *Optical and Quantum Electronics*, **56**,1671(2024).
18. M. K. Halimah, M. A. Hazlin, & F. D. Muhammad, *SpectrochimicaActa Part A: Molecular andBiomolecular Spectroscopy*, **195**,128(2018).

19. R. G. Capelo, R. Santos Baltieri, M. de Oliveira Jr, & D. Manzani, *ACS omega*, 8, 35266 (2023).https://doi.org/10.1021/acsomega.3c05010
20. M. A. Morsy, T. F. Garrison, M. R. Kessler, M. H. Mhareb, & H. Z. El-Deen, *ACS Physical Chemistry Au*, **5**,227(2025).
21. V. Sivaranjani, P. Deepa, P. Murugesan, A. A. Suresh, & M. Dhavamurthy, *Emergent Materials*, **8**, 1(2025).
22. M. P. Hehlen, M. G. Brik, & K. W. Krämer, *Journal of Luminescence*, 136, 221(2013),
23. N. S. Azizan, & M. M. Yusr, *International Journal of Entrepreneurship and Management Practices*, **2**, 93(2019),
24. P. Sailaja, S. Mahamuda, R. A. Talewar, K. Swapna, & A. S. Rao, *Journal of Alloys and Compounds*, **789**, 744(2019),
25. N. Wada & K. Kojima, *Journal of luminescence*, **126**, 53(2007),
26. Y. A. Lakshmi, K. Swapna, K. R. K. Reddy, S. Mahamuda, M. Venkateswarulu,, & A. S. Rao, Optical Materials, **109**, 110328 (2020),
27. P. J. Lakshmi, & K. V. Selvi, *International Journal for Modern Trends in Science and Technology*, **6**,15(2020).
28. K. Damak, C. Rüssel, & R. Maâlej, *Journal of Quantitative Spectroscopy and Radiative Transfer*, **134**,55(2014),
29. Q. Su, Z. Pei, L. Chi, H. Zhang, Z. Zhang, & F. Zou, *Journal of alloys and compounds*, **192**, 25 (1993), https://doi.org/10.1016/0925-8388(93)90174-L
30. W. Thanyaphirak, P. Yasaka, K. Boonin, , N. Sangwaranatee& J. Kaewkhao, *Suranaree Journal of Science & Technology*, **31**,030199(2024).
30. T.Srihari, C.K. Jayasankar, *Optical Materials,***69**, 87(2017),
31. S. Karki, , C. R. Kesavulu H. J. Kim, J. Kaewkhao, N. Chanthima, S. Kothan, & S. Kaewjaeng, *Journal of Non-Crystalline Solids*, **521**,119483(2019)
32. M. Gökçe, & D. Koçyiğit, *Optical Materials*, **89**, 568 (2019)